AIMS Mathematics, 8(6): 13390–13410.
DOI:10.3934/math.2023678
Received: 18 February 2023
Revised: 16 March 2023
Accepted: 20 March 2023
Published: 06 April 2023

http://www.aimspress.com/journal/Math

Research article

Bifurcations and chaotic behavior of a predator-prey model with discrete time

Binhao Hong and Chunrui Zhang*

Department of Mathematics, Northeast Forestry University, Harbin 150040, China

* **Correspondence:** Email: math@nefu.edu.cn; Tel: +8645182190543; Fax: +8645182190543.

Abstract: In this paper, the dynamical behavior of a predator-prey model with discrete time is discussed in terms of both theoretical analysis and numerical simulation. The existence and stability of four equilibria are analyzed. It is proved that the system undergoes Flip bifurcation and Hopf bifurcation around its unique positive equilibrium point using center manifold theorem and bifurcation theory. Additionally, by applying small perturbations to the bifurcation parameter, chaotic cases occur at some corresponding internal equilibria. Finally, numerical simulations are provided with the help of maximum Lyapunov exponent and phase diagrams, which reveal a complex dynamical behavior.

Keywords: predator-prey model; Flip bifurcation; Hopf bifurcation; chaos
Mathematics Subject Classification: 34K18, 37L10, 39A28

1. Introduction

In biology, discrete models of interspecific relationships in populations without generation-level overlap are more generalizable than continuous ones, which has attracted many scholars in recent years (see [1–12]). Obviously, all these works indicate that discrete systems have more complex dynamic behavior. The predator-prey model is a class of classical biomathematical model that has been studied by different scholars in terms of the evolutionary patterns of populations over time [13, 14] and the effects of different functional responses on the stability of populations [15, 16].

For the predator-prey system, external factors such as food supply, climate change and population migration can affect predation and population reproduction [17, 18]. However, the effects of changes in predators themselves are often overlooked, such as predator fear [19]. Frightened predators tend to eat less, which leads to reduced birth rates and increased mortality [19]. Therefore, predator fear, which cannot be quantitatively described, is more difficult to study.

Sasmal [20] studied a predator-prey model with Allee effect and reduced reproduction of prey due

to cost of fear. They discussed the effects of time scale separation between prey and predator.

$$\begin{cases} \frac{du}{dt} = ru\left(1-\frac{u}{k}\right)(u-\theta)\frac{1}{1+fv} - auv & (0<\theta<k) \\ \frac{dv}{dt} = a\alpha uv - mv \end{cases} \tag{1.1}$$

where u and v are the prey and predator population densities, respectively. r is the maximum growth rate of the population, k is the carrying capacity, and θ represents the Allee threshold ($0 < \theta < k$), below which the population becomes extinct. f refers to the level of fear, which is due to the anti-predator response of prey. a is the predation rate, α is the conversion efficiency of predator by consuming prey, and m represents the predator's natural mortality rate.

To simplify parameters, define $N = \frac{u}{k}$, $P = \frac{a}{rk}v$, $\epsilon = \frac{a\alpha}{r}$, $\theta = \frac{\theta}{k}$, $m = \frac{m}{a\alpha k}$, $f = \frac{rkf}{a}$, $t = a\alpha kt$. Then, the system is given by

$$\begin{cases} \frac{dN}{dt} = \frac{1}{\epsilon}\left[N(1-N)(N-\theta)\frac{1}{1+fP} - NP\right] \\ \frac{dP}{dt} = NP - mP \end{cases}$$

At present, there are some studies on predator-prey systems with Flip bifurcation and Hopf bifurcation [21] in continuous models, where, however, the chaotic properties have not been mentioned. For example, Khan studied a discrete-time Nicholson-Bailey host-parasitoid model and obtained the local dynamics and supercritical Neimark-Sacker bifurcation in 2017 [22]. In 2019, Li et al. investigated the discrete time predator-prey model undergoing Flip and Neimark Sacker bifurcation using the center manifold theorem and bifurcation theory [23]. In 2022, Yu et al. gave a description of the bifurcations in theory for a symmetrically coupled period-doubling system, including the Transcritical bifurcation, Pitchfork bifurcation, Flip bifurcation and Neimark-Sacker bifurcation [24]. In 2022, Chen et al. studied a discrete predator-prey system with Allee effect, which undergoes Fold bifurcation and Flip bifurcation. They obtained cascades of period-doubling bifurcation in orbits of period-2, 4, 8 and chaotic properties [25].

Based on the above analysis and discussion, we obtain the following discrete-time model:

$$\begin{cases} N_{n+1} = N_n + h\left\{\frac{1}{\epsilon}\left[N_n(1-N_n)(N_n-\theta)\frac{1}{1+fP_n} - N_nP_n\right]\right\} \\ P_{n+1} = P_n + h\left[N_nP_n - mP_n\right] \end{cases} \tag{1.2}$$

where $h > 0$ refers to the step length of (1.2), $0 < \theta < 1$.

In this paper, we study the existence and stability of four equilibria of model (1.2) and focus on local dynamics of the unique positive equilibrium point in Section 2 . In Sections 3 and 4, we study Flip bifurcation and Hopf bifurcation when bifurcation parameter h varies in a small neighborhood of the unique positive equilibrium point. In Section 5, we study chaos scenarios of Flip bifurcation. Meanwhile, some numerical simulations about bifurcations are given by maximum Lyapunov exponent and phase diagrams to verify our results. Finally, brief conclusions are given in Section 6.

2. Existence and stability of equilibria

Initially, the existence and stability of the equilibrium point of model (1.2) are analyzed.

By calculating model (1.2), obviously, the trivial equilibrium point $E_1 = (0, 0)$ and boundary equilibria $E_2 = (1, 0)$, $E_3 = (\theta, 0)$ are obtained. Since the negative equilibrium point has no practical

meaning in biology, the unique positive internal equilibrium point $E_4 = \left(m, \frac{-1+\sqrt{1+4f(1-m)(m-\theta)}}{2f}\right)$ is chosen.

The Jacobi matrix of the linear system of (1.2) at any equilibrium point (N^*, P^*) is given by:

$$J = \begin{pmatrix} 1+\frac{h}{\epsilon}\left[\frac{-3N^2+2(1+\theta)N-\theta}{1+fP} - P\right] & \frac{h}{\epsilon}\left[\left(N^3-(1+\theta)N^2+\theta N\right)\frac{f}{(1+fP)^2} - N\right] \\ hP & 1+hN-mh \end{pmatrix}\Bigg|_{(N^*,P^*)}$$

Now, we give some dynamical properties of four equilibria.

Theorem 2.1. *For the trivial equilibrium E_1, with eigenvalues $\lambda_1 = 1-\frac{h\theta}{\epsilon}$ and $\lambda_2 = 1-hm$.*

(i) E_1 is a sink if $0 < h < \min\left\{\frac{2\epsilon}{\theta}, \frac{2}{m}\right\}$, with eigenvalues $|\lambda_1| < 1$ and $|\lambda_2| < 1$.

(ii) E_1 is a source if $h > \max\left\{\frac{2\epsilon}{\theta}, \frac{2}{m}\right\}$, with eigenvalues $|\lambda_1| > 1$ and $|\lambda_2| > 1$.

(iii) E_1 is a saddle point if $\frac{2\epsilon}{\theta} < h < \frac{2}{m}$ with eigenvalues $|\lambda_1| > 1$ and $|\lambda_2| < 1$, or $\frac{2}{m} < h < \frac{2\epsilon}{\theta}$ with eigenvalues $|\lambda_1| < 1$ and $|\lambda_2| > 1$.

(iv) Flip bifurcation occurs at E_1 if $h = \frac{2\epsilon}{\theta} < \frac{2}{m}$, with eigenvalues $\lambda_1 = -1$ and $|\lambda_2| < 1$, or $h = \frac{2}{m} < \frac{2\epsilon}{\theta}$, with eigenvalues $\lambda_2 = -1$ and $|\lambda_1| < 1$.

Theorem 2.2. *For the boundary equilibrium E_2, with eigenvalues $\lambda_1 = 1+\frac{h}{\epsilon}(\theta-1)$ and $\lambda_2 = 1+h(1-m)$.*

(i) E_2 is a sink if $\begin{cases} m>1 \\ 0<h<\min\left(\frac{2\epsilon}{1-\theta}, \frac{2}{m-1}\right) \end{cases}$, with eigenvalues $|\lambda_1| < 1$ and $|\lambda_2| < 1$.

(ii) E_2 is a source if $\begin{cases} m<1 \\ h>\frac{2\epsilon}{1-\theta} \end{cases}$ or $\begin{cases} m>1 \\ h>\max\left\{\frac{2\epsilon}{1-\theta}, \frac{2}{m-1}\right\} \end{cases}$, with eigenvalues $|\lambda_1| > 1$ and $|\lambda_2| > 1$.

(iii) E_2 is a saddle point if $\begin{cases} m>1 \\ \frac{2\epsilon}{1-\theta}<h<\frac{2}{m-1} \end{cases}$ or $\begin{cases} m>1 \\ \frac{2}{m-1}<h<\frac{2\epsilon}{1-\theta} \end{cases}$ with eigenvalues $|\lambda_1| > 1$ and $|\lambda_2| < 1$, or $\begin{cases} m<1 \\ h<\frac{2\epsilon}{1-\theta} \end{cases}$ with eigenvalues $|\lambda_1| < 1$ and $|\lambda_2| > 1$.

(iv) Flip bifurcation occurs at E_2 if $\begin{cases} m>1 \\ h=\frac{2\epsilon}{1-\theta}<\frac{2}{m-1} \end{cases}$ with eigenvalues $\lambda_1 = -1$ and $|\lambda_2| < 1$, or $h = \frac{2}{m-1} < \frac{2\epsilon}{1-\theta}$ with eigenvalues $\lambda_2 = -1$ and $|\lambda_1| < 1$.

(v) Transcritical bifurcation occurs at E_2 if $\begin{cases} m=1 \\ h<\frac{2\epsilon}{1-\theta} \end{cases}$, with eigenvalues $\lambda_2 = 1$ and $|\lambda_1| < 1$.

Theorem 2.3. *For the equilibrium E_3, with eigenvalues $\lambda_1 = 1+\frac{h}{\epsilon}\theta(1-\theta)$ and $\lambda_2 = 1+h(\theta-m)$.*

(i) E_3 is a source if $\theta > m$ or $\begin{cases} \theta<m \\ h>\frac{2}{m-\theta} \end{cases}$, with eigenvalues $|\lambda_1| > 1$ and $|\lambda_2| > 1$.

(ii) E_3 is a saddle point if $\begin{cases} \theta<m \\ 0<h<\frac{2}{m-\theta} \end{cases}$, with eigenvalues $|\lambda_1| > 1$ and $|\lambda_2| < 1$.

There is no situation as $|\lambda_1| < 1$, i.e., stability does not exist.

Theorem 2.4. *For the internal equilibrium E_4,*

(i) E_4 is a sink if

$$\begin{cases} 1+\frac{h}{\epsilon}\left[\frac{m(1+\theta-2m)}{1+\sqrt{1+4f(1-m)(m-\theta)}}\right] + \frac{h^2}{\epsilon}\left[\frac{m(1-m)(m-\theta)\sqrt{1+4f(1-m)(m-\theta)}}{\left[1+\sqrt{1+4f(1-m)(m-\theta)}\right]^2}\right] > 0 \\ m(1-m)(m-\theta)\sqrt{1+4f(1-m)(m-\theta)} > 0 \\ \frac{1+\theta-2m}{1+\sqrt{1+4f(1-m)(m-\theta)}} + h\left[\frac{2(1-m)(m-\theta)\sqrt{1+4f(1-m)(m-\theta)}}{\left[1+\sqrt{1+4f(1-m)(m-\theta)}\right]^2}\right] < 0 \end{cases}$$

(*ii*) *Transcritical bifurcation occurs at* E_4 *if*

$$\begin{cases} m = 1 \text{ or } m = \theta \\ -2\epsilon < h\left[\frac{2m(1+\theta-2m)}{1+\sqrt{1+4f(1-m)(m-\theta)}}\right] < 0. \end{cases}$$

(*iii*) *Flip bifurcation occurs at* E_4 *if*

$$\begin{cases} 1 + \frac{h}{\epsilon}\left[\frac{m(1+\theta-2m)}{1+\sqrt{1+4f(1-m)(m-\theta)}}\right] + \frac{h^2}{\epsilon}\left[\frac{m(1-m)(m-\theta)\sqrt{1+4f(1-m)(m-\theta)}}{\left[1+\sqrt{1+4f(1-m)(m-\theta)}\right]^2}\right] = 0 \\ -4 < \frac{h}{\epsilon}\left[\frac{m(1+\theta-2m)}{1+\sqrt{1+4f(1-m)(m-\theta)}}\right] < -2. \end{cases}$$

(*iv*) *Hopf bifurcation occurs at* E_4 *if*

$$\begin{cases} h = \frac{(2m-\theta-1)\left[1+\sqrt{1+4f(1-m)(m-\theta)}\right]}{2(1-m)(m-\theta)\sqrt{1+4f(1-m)(m-\theta)}} \\ -4 < \frac{h}{\epsilon}\left[\frac{m(1+\theta-2m)}{1+\sqrt{1+4f(1-m)(m-\theta)}}\right] < 0. \end{cases}$$

Proof. The Jacobi matrix of (1.2) at point $E_4 = (N_0, P_0)$ is

$$J|_{(N_0,P_0)} = \begin{pmatrix} 1 + \frac{h}{\epsilon}\left[\frac{2m(1+\theta-2m)}{1+\sqrt{1+4f(1-m)(m-\theta)}}\right] & \frac{h}{\epsilon}\left[\frac{-2m+\sqrt{1+4f(1-m)(m-\theta)}}{1+\sqrt{1+4f(1-m)(m-\theta)}}\right] \\ \frac{h\left(-1+\sqrt{1+4f(1-m)(m-\theta)}\right)}{2f} & 1 \end{pmatrix} \tag{2.1}$$

where $n = 1 + \sqrt{1 + 4f(1-m)(m-\theta)}$.

Meanwhile, the characteristic polynomial of $J|_{(N_0,P_0)}$ is given by:

$$f(\lambda) = \lambda^2 - (A+1)\lambda + (A + BC) = 0 \tag{2.2}$$

where

$$A = 1 + \frac{h}{\epsilon}\left[\frac{2m(1+\theta-2m)}{1+\sqrt{1+4f(1-m)(m-\theta)}}\right],$$

$$B = \frac{h}{\epsilon}\left[\frac{-2m+\sqrt{1+4f(1-m)(m-\theta)}}{1+\sqrt{1+4f(1-m)(m-\theta)}}\right], \quad C = \frac{h\left(-1+\sqrt{1+4f(1-m)(m-\theta)}\right)}{2f}.$$

Then, eigenvalues of $J|_{(N_0,P_0)}$ are $\lambda_1 = \frac{A+1+\sqrt{\Delta}}{2}$ and $\lambda_2 = \frac{A+1-\sqrt{\Delta}}{2}$, where $\Delta = (A-1)^2 - 4BC$.

(*i*) (N_0, P_0) is a sink, if $|\lambda_1| < 1$ and $|\lambda_2| < 1$. From the Jury Criterion [26], we obtain $\begin{cases} 1 + (A+1) + (A+BC) > 0 \\ 1 - (A+1) + (A+BC) > 0 \\ 1 - (A+BC) > 0 \end{cases}$.

(*ii*) If $\Delta > 0$, $\lambda_1 = 1$ and $|\lambda_2| < 1$ or $\lambda_2 = 1$ and $|\lambda_1| < 1$, then we have $\begin{cases} BC = 0 \\ |A| < 1 \end{cases}$.

(*iii*) If $\Delta > 0$, $\lambda_1 = -1$ and $|\lambda_2| < 1$ or $\lambda_2 = -1$ and $|\lambda_1| < 1$, then we have $\begin{cases} 2A + BC + 2 = 0 \\ |A + 2| < 1 \end{cases}$.

(*iv*) If $\Delta < 0$, $|\lambda_1| = |\lambda_2| = 1$, which is a pair of conjugate complex roots, then we have $\begin{cases} A + BC = 1 \\ 0 < |A + 1| < 2 \end{cases}$.

When λ_1 and λ_2 is a pair of conjugate complex roots, we assume $\lambda_1 = a + bi$ and $\lambda_2 = a - bi$ $\left(a^2 + b^2 = 1\ ,\ b \neq 0\right)$, *i.e.*, $0 < |a| < 1$. Since $(\lambda - \lambda_1)(\lambda - \lambda_2) = \lambda^2 - (\lambda_1 + \lambda_2)\lambda + \lambda_1\lambda_2 = 0$, obviously we have $\lambda_1 + \lambda_2 = A + 1 = 2a$ and $\lambda_1\lambda_2 = A + BC = 1$.

All of the expressions A, B, C can be brought into equations mentioned above to obtain the corresponding conclusions. □

3. Flip bifurcation at E_4

In this section, we discuss how system (1.2) undergoes Flip bifurcation around its internal equilibrium $E_4 = \left(m, \frac{-1+\sqrt{1+4f(1-m)(m-\theta)}}{2f}\right)$ when h is chosen as bifurcation parameter. The necessary conditions for Flip bifurcation to occur is given by the following curve:

$$U = \left\{ (m, n, \theta, f, \epsilon) \in \mathbb{R}_+^5 :\ h = h^* = \frac{2f(2m-1-\theta) + 2\sqrt{f^2(1+\theta-2m)^2 + \frac{1}{m}(n-1)(n-2)\epsilon f n}}{m(n-1)(n-2)}\ ,\ |D| < 1 \right\}$$

where $D = \frac{h}{\epsilon}\left(\frac{m(1+\theta-2m)}{1+\sqrt{1+4f(1-m)(m-\theta)}}\right) + 3$ and $n = 1 + \sqrt{1 + 4f(1-m)(m-\theta)}$.

3.1. Existence condition of Flip bifurcation at E_4

The Jacobi matrix of the linear system of (1.2) at the equilibrium point (N_0, P_0) is given by:

$$J|_{(N_0,P_0)} = \begin{pmatrix} 1 + \frac{h}{\epsilon}\left[\frac{2m(1+\theta-2m)}{n}\right] & \frac{h}{\epsilon}\left[\frac{-2m(n-1)}{n}\right] \\ \frac{h(n-2)}{2f} & 1 \end{pmatrix} \tag{3.1}$$

where $n = 1 + \sqrt{1 + 4f(1-m)(m-\theta)}$.

In order to obtain the bifurcation properties, we consider translations $\overline{N_{n+1}} = N_{n+1} - N_0$, $\overline{P_{n+1}} = P_{n+1} - P_0$ for shifting (N_0, P_0) to the origin. Then, the model (1.2) is given by

$$\begin{cases} \overline{N_{n+1}} = \overline{N_n} + h\left\{\frac{1}{\epsilon}\left[\left(\overline{N_n} + N_0\right)\left(1 - \overline{N_n} - N_0\right)\left(\overline{N_n} + N_0 - \theta\right)\frac{1}{1+f\left(\overline{P_n}+P_0\right)} - \left(\overline{N_n} + N_0\right)\left(\overline{P_n} + P_0\right)\right]\right\} \\ \overline{P_{n+1}} = \overline{P_n} + h\left[\left(\overline{N_n} + N_0\right)\left(\overline{P_n} + P_0\right) - m\left(\overline{P_n} + P_0\right)\right] \end{cases} \tag{3.2}$$

Using Taylor expansion at the point $E_4(N_0, P_0)$ yields the following expression :

$$\begin{pmatrix} \overline{N_{n+1}} \\ \overline{P_{n+1}} \end{pmatrix} = J|_{(N_0,P_0)} \begin{pmatrix} \overline{N_n} \\ \overline{P_n} \end{pmatrix} + h \begin{pmatrix} \frac{1}{\epsilon}\psi_1\left(\overline{N_n}, \overline{P_n}\right) \\ \psi_2\left(\overline{N_n}, \overline{P_n}\right) \end{pmatrix} \tag{3.3}$$

where

$$\psi_1\left(\overline{N_n}, \overline{P_n}\right) = b_1\overline{N_n}^2 + b_2\overline{N_n P_n} + b_3\overline{P_n}^2 + b_4\overline{N_n}^3 + b_5\overline{N_n}^2\overline{P_n} + b_6\overline{N_n}\,\overline{P_n}^2 + b_7\overline{P_n}^3 + O\left(\left(\left|\overline{N_n}\right| + \left|\overline{P_n}\right|\right)^4\right),$$

$$\psi_2\left(\overline{N_n}, \overline{P_n}\right) = \overline{N_n}\,\overline{P_n},$$

$b_1 = \frac{-3N_0+1+\theta}{1+fP_0}$, $b_2 = \frac{\left[3N_0^2-2(1+\theta)N_0+\theta\right]f}{(1+fP_0)^2} - 1$, $b_3 = \frac{\left[-N_0^3+(1+\theta)N_0^2-\theta N_0\right]f^2}{(1+fP_0)^3}$, $b_4 = \frac{-1}{1+fP_0}$, $b_5 = \frac{(3N_0-1-\theta)f}{(1+fP_0)^2}$,

$b_6 = \frac{\left[3N_0^2-2(1+\theta)N_0+\theta\right]f^2}{(1+fP_0)^3}$, $b_7 = \frac{\left[N_0^3-(1+\theta)N_0^2+\theta N_0\right]f^3}{(1+fP_0)^4}$.

From the characteristic polynomial (2.2), we obtain $f(-1) = \frac{h^2}{\epsilon}\left[\frac{m(n-1)(n-2)}{fn}\right] + \frac{h}{\epsilon}\left[\frac{4m(1+\theta-2m)}{n}\right] + 4$. Since step size $h > 0$, the bifurcation parameter is chosen as

$$h^* = \frac{2f(2m-1-\theta) + 2\sqrt{f^2(1+\theta-2m)^2 + \frac{1}{m}(n-1)(n-2)\epsilon fn}}{m(n-1)(n-2)}$$

where parameter m satisfies $\frac{1+\theta}{2} < m < 1$.

Consider parameter h with a small perturbation δ, i.e., $h = h^* + \delta$, $|\delta| \ll 1$, and the system (3.3) becomes

$$\begin{pmatrix} \overline{N_{n+1}} \\ \overline{P_{n+1}} \end{pmatrix} = \begin{pmatrix} 1 + \frac{(h^*+\delta)}{\epsilon}\left[\frac{2m(1+\theta-2m)}{n}\right] & \frac{(h^*+\delta)}{\epsilon}\left[\frac{-2m(n-1)}{n}\right] \\ \frac{(h^*+\delta)(n-2)}{2f} & 1 \end{pmatrix}\begin{pmatrix} \overline{N_n} \\ \overline{P_n} \end{pmatrix} + (h^*+\delta)\begin{pmatrix} \frac{1}{\epsilon}\psi_1\left(\overline{N_n}, \overline{P_n}\right) \\ \psi_2\left(\overline{N_n}, \overline{P_n}\right) \end{pmatrix} \tag{3.4}$$

The characteristic polynomial of (3.4) is given by

$$g(\lambda) = \lambda^2 - \left[2 + \frac{h^*+\delta}{\epsilon}\left[\frac{2m(1+\theta-2m)}{n}\right]\right]\lambda + 1 + \frac{h^*+\delta}{\epsilon}\left[\frac{2m(1+\theta-2m)}{n}\right] + \frac{(h^*+\delta)^2}{\epsilon}\left[\frac{m(n-1)(n-2)}{fn}\right]$$

The transversal condition at (N_0, P_0) is

$$\frac{dg(\lambda)}{d\delta}\Big|_{\lambda=-1,\delta=0} = -4 - \frac{2mh^*(1+\theta-2m)}{\epsilon n}$$

If $\frac{dg(\lambda)}{d\delta}\Big|_{\lambda=-1,\delta=0} \neq 0$, then Flip bifurcation will occur at E_4.

3.2. *The direction of Flip bifurcation at E_4*

To facilitate discussion, define $A = \begin{pmatrix} 1 + \frac{h^*}{\epsilon}\left[\frac{2m(1+\theta-2m)}{n}\right] & \frac{h^*}{\epsilon}\left[\frac{-2m(n-1)}{n}\right] \\ \frac{h^*(n-2)}{2f} & 1 \end{pmatrix}$.

If the eigenvalue of A goes for $\lambda = -1$, the corresponding eigenvector is given as:

$$T_1 = \begin{pmatrix} \frac{h^*}{\epsilon}\left[\frac{-2m(n-1)}{n}\right] \\ -2 - \frac{h^*}{\epsilon}\left[\frac{2m(1+\theta-2m)}{n}\right] \end{pmatrix}$$

If the eigenvalue of A goes for $\lambda = \lambda_2$, the corresponding eigenvector is given as:

$$T_2 = \begin{pmatrix} \frac{h^*}{\epsilon}\left[\frac{-2m(n-1)}{n}\right] \\ \lambda_2 - 1 - \frac{h^*}{\epsilon}\left[\frac{2m(1+\theta-2m)}{n}\right] \end{pmatrix}$$

Then, we have the invertible matrix

$$T = \left(T_1, T_2\right) = \begin{pmatrix} \frac{h^*}{\epsilon}\left[\frac{-2m(n-1)}{n}\right] & \frac{h^*}{\epsilon}\left[\frac{-2m(n-1)}{n}\right] \\ -2 - \frac{h^*}{\epsilon}\left[\frac{2m(1+\theta-2m)}{n}\right] & \lambda_2 - 1 - \frac{h^*}{\epsilon}\left[\frac{2m(1+\theta-2m)}{n}\right] \end{pmatrix}$$

Using translation $\begin{pmatrix} x_n \\ y_n \end{pmatrix} = T^{-1}\begin{pmatrix} \overline{N_n} \\ \overline{P_n} \end{pmatrix}$, system (3.4) turns into

$$\begin{pmatrix} x_{n+1} \\ y_{n+1} \end{pmatrix} = \begin{pmatrix} -1 & 0 \\ 0 & \lambda_2 \end{pmatrix}\begin{pmatrix} x_n \\ y_n \end{pmatrix} + \begin{pmatrix} f_1\left(\overline{N_n}, \overline{P_n}, \delta\right) \\ g_1\left(\overline{N_n}, \overline{P_n}, \delta\right) \end{pmatrix} \tag{3.5}$$

where

$$\begin{aligned} f_1\left(\overline{N_n}, \overline{P_n}, \delta\right) &= a_{11}\overline{N_n}\delta + a_{12}\overline{P_n}\delta + b_{11}\overline{N_n}^2 + b_{12}\overline{N_n}\,\overline{P_n} + b_{13}\overline{P_n}^2 + b_{14}\overline{N_n}^3 + b_{15}\overline{N_n}^2\overline{P_n} + b_{16}\overline{N_n}\,\overline{P_n}^2 \\ &\quad + b_{17}\overline{P_n}^3 + c_{11}\overline{N_n}^2\delta + c_{12}\overline{N_n}\,\overline{P_n}\delta + c_{13}\overline{P_n}^2\delta + c_{14}\overline{N_n}^3\delta + c_{15}\overline{N_n}^2\overline{P_n}\delta + c_{16}\overline{N_n}\,\overline{P_n}^2\delta \\ &\quad + c_{17}\overline{P_n}^3\delta \end{aligned}$$

$$\begin{aligned} g_1\left(\overline{N_n}, \overline{P_n}, \delta\right) &= a_{21}\overline{N_n}\delta + a_{22}\overline{P_n}\delta + b_{21}\overline{N_n}^2 + b_{22}\overline{N_n}\,\overline{P_n} + b_{23}\overline{P_n}^2 + b_{24}\overline{N_n}^3 + b_{25}\overline{N_n}^2\overline{P_n} + b_{26}\overline{N_n}\,\overline{P_n}^2 \\ &\quad + b_{27}\overline{P_n}^3 + c_{21}\overline{N_n}^2\delta + c_{22}\overline{N_n}\,\overline{P_n}\delta + c_{23}\overline{P_n}^2\delta + c_{24}\overline{N_n}^3\delta + c_{25}\overline{N_n}^2\overline{P_n}\delta + c_{26}\overline{N_n}\,\overline{P_n}^2\delta \\ &\quad + c_{27}\overline{P_n}^3\delta \end{aligned}$$

$$\begin{aligned} a_{11} &= \frac{1}{h^*(\lambda_2+1)}\left[\frac{2m-1-\theta}{n-1}\right]\left(\lambda_2 - 1 - \frac{h^*}{\epsilon}\left[\frac{2m(1+\theta-2m)}{n}\right]\right) - \frac{n-2}{2f(\lambda_2+1)} \\ a_{12} &= \frac{1}{h^*(\lambda_2+1)}\left(\lambda_2 - 1 - \frac{h^*}{\epsilon}\left[\frac{2m(1+\theta-2m)}{n}\right]\right) \\ a_{21} &= \frac{1}{h^*(\lambda_2+1)}\left[\frac{2m-1-\theta}{n-1}\right]\left(2 + \frac{h^*}{\epsilon}\left[\frac{2m(1+\theta-2m)}{n}\right]\right) + \frac{n-2}{2f(\lambda_2+1)} \\ a_{22} &= \frac{1}{h^*(\lambda_2+1)}\left(2 + \frac{h^*}{\epsilon}\left[\frac{2m(1+\theta-2m)}{n}\right]\right) \\ b_{11} &= \frac{1}{\lambda_2+1}\left[\frac{n}{-2m(n-1)}\right]\left(\lambda_2 - 1 - \frac{h^*}{\epsilon}\left[\frac{2m(1+\theta-2m)}{n}\right]\right)b_1 \\ b_{12} &= \frac{1}{\lambda_2+1}\left[\frac{n}{-2m(n-1)}\right]\left(\lambda_2 - 1 - \frac{h^*}{\epsilon}\left[\frac{2m(1+\theta-2m)}{n}\right]\right)b_2 - \frac{h^*}{\lambda_2+1} \\ b_{13} &= \frac{1}{\lambda_2+1}\left[\frac{n}{-2m(n-1)}\right]\left(\lambda_2 - 1 - \frac{h^*}{\epsilon}\left[\frac{2m(1+\theta-2m)}{n}\right]\right)b_3 \\ &\vdots \\ b_{17} &= \frac{1}{\lambda_2+1}\left[\frac{n}{-2m(n-1)}\right]\left(\lambda_2 - 1 - \frac{h^*}{\epsilon}\left[\frac{2m(1+\theta-2m)}{n}\right]\right)b_7 \\ c_{ij} &= h^* b_{ij} \quad (i = 1, 2\ ;\ j = 1, 2, \cdots, 7) \end{aligned}$$

Using translation $\begin{pmatrix} \overline{N_{n+1}} \\ \overline{P_{n+1}} \end{pmatrix} = T \begin{pmatrix} x_{n+1} \\ y_{n+1} \end{pmatrix}$, system (3.5) becomes

$$\begin{pmatrix} x_{n+1} \\ y_{n+1} \end{pmatrix} = \begin{pmatrix} -x_n \\ \lambda_2 y_n \end{pmatrix} + \begin{pmatrix} f_2(x_n, y_n, \delta) \\ g_2(x_n, y_n, \delta) \end{pmatrix} \tag{3.6}$$

where

$$\begin{aligned} f_2(x_n, y_n, \delta) = {} & d_{11}x_n\delta + d_{12}y_n\delta + e_{11}x_n^2 + e_{12}x_ny_n + e_{13}y_n^2 + e_{14}x_n^3 + e_{15}x_n^2y_n + e_{16}x_ny_n^2 \\ & + e_{17}y_n^3 + f_{11}x_n^2\delta + f_{12}x_ny_n\delta + f_{13}y_n^2\delta + f_{14}x_n^3\delta + f_{15}x_n^2y_n\delta + f_{16}x_ny_n^2\delta \\ & + f_{17}y_n^3\delta \end{aligned}$$

$$\begin{aligned} g_2(x_n, y_n, \delta) = {} & d_{21}x_n\delta + d_{22}y_n\delta + e_{21}x_n^2 + e_{22}x_ny_n + e_{23}y_n^2 + e_{24}x_n^3 + e_{25}x_n^2y_n + e_{26}x_ny_n^2 \\ & + e_{27}y_n^3 + f_{21}x_n^2\delta + f_{22}x_ny_n\delta + f_{23}y_n^2\delta + f_{24}x_n^3\delta + f_{25}x_n^2y_n\delta + f_{26}x_ny_n^2\delta \\ & + f_{27}y_n^3\delta \end{aligned}$$

$$k_{11} = k_{12} = \tfrac{h^*}{\epsilon}\left[\tfrac{-2m(n-1)}{n}\right],\ k_{21} = -2 - \tfrac{h^*}{\epsilon}\left[\tfrac{2m(1+\theta-2m)}{n}\right],\ k_{22} = \lambda_2 - 1 - \tfrac{h^*}{\epsilon}\left[\tfrac{2m(1+\theta-2m)}{n}\right]$$

$$\begin{aligned} & d_{11} = a_{11}k_{11} + a_{12}k_{21},\ d_{12} = a_{11}k_{12} + a_{12}k_{22},\ e_{11} = b_{11}k_{11}^2 + b_{12}k_{11}k_{21} + b_{13}k_{21}^2, \\ & e_{12} = 2b_{11}k_{11}k_{12} + b_{12}(k_{11}k_{22} + k_{12}k_{21}) + 2b_{13}k_{21}k_{22},\ e_{13} = b_{11}k_{12}^2 + b_{12}k_{12}k_{22} + b_{13}k_{22}^2, \\ & e_{14} = b_{14}k_{11}^3 + b_{15}k_{11}^2k_{21} + b_{16}k_{11}k_{21}^2 + b_{17}k_{21}^3, \\ & e_{15} = 3b_{14}k_{11}^2k_{12} + b_{15}\left(k_{11}^2k_{22} + 2k_{11}k_{12}k_{21}\right) + b_{16}\left(2k_{11}k_{21}k_{22} + k_{12}k_{21}^2\right) + 3b_{17}k_{21}^2k_{22}, \\ & e_{16} = 3b_{14}k_{11}k_{12}^2 + b_{15}\left(2k_{11}k_{12}k_{22} + k_{12}^2k_{21}\right) + b_{16}\left(k_{11}k_{22}^2 + 2k_{12}k_{21}k_{22}\right) + 3b_{17}k_{21}k_{22}^2, \\ & e_{17} = b_{14}k_{12}^3 + b_{15}k_{12}^2k_{22} + b_{16}k_{12}k_{22}^2 + b_{17}k_{22}^3, \\ & d_{21} = a_{21}k_{11} + a_{22}k_{21},\ d_{22} = a_{21}k_{12} + a_{22}k_{22},\ e_{21} = b_{21}k_{11}^2 + b_{22}k_{11}k_{21} + b_{23}k_{21}^2, \\ & e_{22} = 2b_{21}k_{11}k_{12} + b_{22}(k_{11}k_{22} + k_{12}k_{21}) + 2b_{23}k_{21}k_{22},\ e_{23} = b_{21}k_{12}^2 + b_{22}k_{12}k_{22} + b_{23}k_{22}^2, \\ & e_{24} = b_{24}k_{11}^3 + b_{25}k_{11}^2k_{21} + b_{26}k_{11}k_{21}^2 + b_{27}k_{21}^3, \\ & e_{25} = 3b_{24}k_{11}^2k_{12} + b_{25}\left(k_{11}^2k_{22} + 2k_{11}k_{12}k_{21}\right) + b_{26}\left(2k_{11}k_{21}k_{22} + k_{12}k_{21}^2\right) + 3b_{27}k_{21}^2k_{22}, \\ & e_{26} = 3b_{24}k_{11}k_{12}^2 + b_{25}\left(2k_{11}k_{12}k_{22} + k_{12}^2k_{21}\right) + b_{26}\left(k_{11}k_{22}^2 + 2k_{12}k_{21}k_{22}\right) + 3b_{27}k_{21}k_{22}^2, \\ & e_{27} = b_{24}k_{12}^3 + b_{25}k_{12}^2k_{22} + b_{26}k_{12}k_{22}^2 + b_{27}k_{22}^3, \\ & f_{ij} = he_{ij} \quad (i = 1, 2\ ;\ j = 1, 2, \cdots, 7)\,. \end{aligned}$$

Next, by using the center manifold theorem and normal form theories, the direction of Flip bifurcation at E_4 is given.

$$\alpha_1 = \left(\frac{\partial^2 f}{\partial \tilde{x}_n \delta} + \frac{1}{2}\frac{\partial f}{\partial \delta}\frac{\partial^2 f}{\partial \tilde{x}_n^2}\right)|_{(0,0)}, \qquad \alpha_2 = \left(\frac{1}{6}\frac{\partial^3 f}{\partial \tilde{x}_n^3} + \left(\frac{1}{2}\frac{\partial^2 f}{\partial \tilde{x}_n^2}\right)^2\right)|_{(0,0)},$$

where the coefficients of α_1 and α_2 are derived from (3.6).

Theorem 3.1. *If $\alpha_1 \neq 0$, $\alpha_2 \neq 0$, then the system undergoes Flip bifurcation at the immobile point (N_0, P_0), and if $\alpha_2 > 0\,(< 0)$, then the two-cycle point is stable (unstable).*

For sufficiently small neighborhoods of the parameter $\delta = 0$, there exists a central manifold at $(0, 0)$:

$$W^c(0,0) = \left\{ (\tilde{x}, \tilde{y}) : \tilde{y}_{n+1} = m_1\tilde{x}_{n+1}^2 + m_2\tilde{x}_{n+1}\delta \right\} \tag{3.7}$$

Substituting (3.7) into (3.6), the solution is given as

$$m_1 = \frac{e_{21}}{1-\lambda_2} = \frac{b_{21}k_{11}^2 + b_{22}k_{11}k_{21} + b_{23}k_{21}^2}{1-\lambda_2}, \qquad m_2 = \frac{-d_{21}}{1+\lambda_2} = \frac{-(a_{21}k_{11} + a_{22}k_{21})}{1+\lambda_2}$$

Restricting the system of equations on $W^c(0,0)$, the results are as follows.

$$\tilde{x}_{n+1} = -\tilde{x}_n + l_1\tilde{x}_n^2 + l_2\tilde{x}_n\delta + l_3\tilde{x}_n^2\delta + l_4\tilde{x}_n\delta^2 + l_5\tilde{x}_n^3 + O\left((|\tilde{x}_n| + |\delta|)^4\right)$$

where $l_1 = e_{11} = b_{11}k_{11}^2 + b_{12}k_{11}k_{21} + b_{13}k_{21}^2$, $l_2 = d_{11} = a_{11}k_{11} + a_{12}k_{21}$, $l_3 = d_{12}m_1 + f_{11} + e_{12}m_2$, $l_4 = d_{12}m_2$, $l_5 = e_{12}m_1 + e_{14}$.

According to the normal form theories related to bifurcation analysis, we require the following quantity at $(x, y, \delta) = (0, 0, 0)$.

$$\alpha_1 = \left(\frac{\partial^2 f}{\partial\tilde{x}_n\delta} + \frac{1}{2}\frac{\partial f}{\partial\delta}\frac{\partial^2 f}{\partial\tilde{x}_n^2}\right)|_{(0,0)} = l_2 + l_3, \qquad \alpha_2 = \left(\frac{1}{6}\frac{\partial^3 f}{\partial\tilde{x}_n^3} + \left(\frac{1}{2}\frac{\partial^2 f}{\partial\tilde{x}_n^2}\right)^2\right)|_{(0,0)} = l_5 + l_1^2$$

For numerical simulations, we choose the following parameters to prove our theoretical discussion. The unique positive equilibrium point $(N_0, P_0) \approx (0.89, 0.0708765)$ of the model can be obtained by giving the parameters $h = 0.1$, $e = 0.023933614$, $\theta = 0.2$, $f = 1$, $m = 0.89$. By choosing the initial value of $(0.9, 0.07115)$, the result can be obtained by numerical simulation as Figure 1.

It is obvious from the diagrams that variables N and P appear as two-point solutions with a period for a given parameter condition and gradually stabilize near the equilibrium point, which verifies Flip bifurcation occurs at this point.

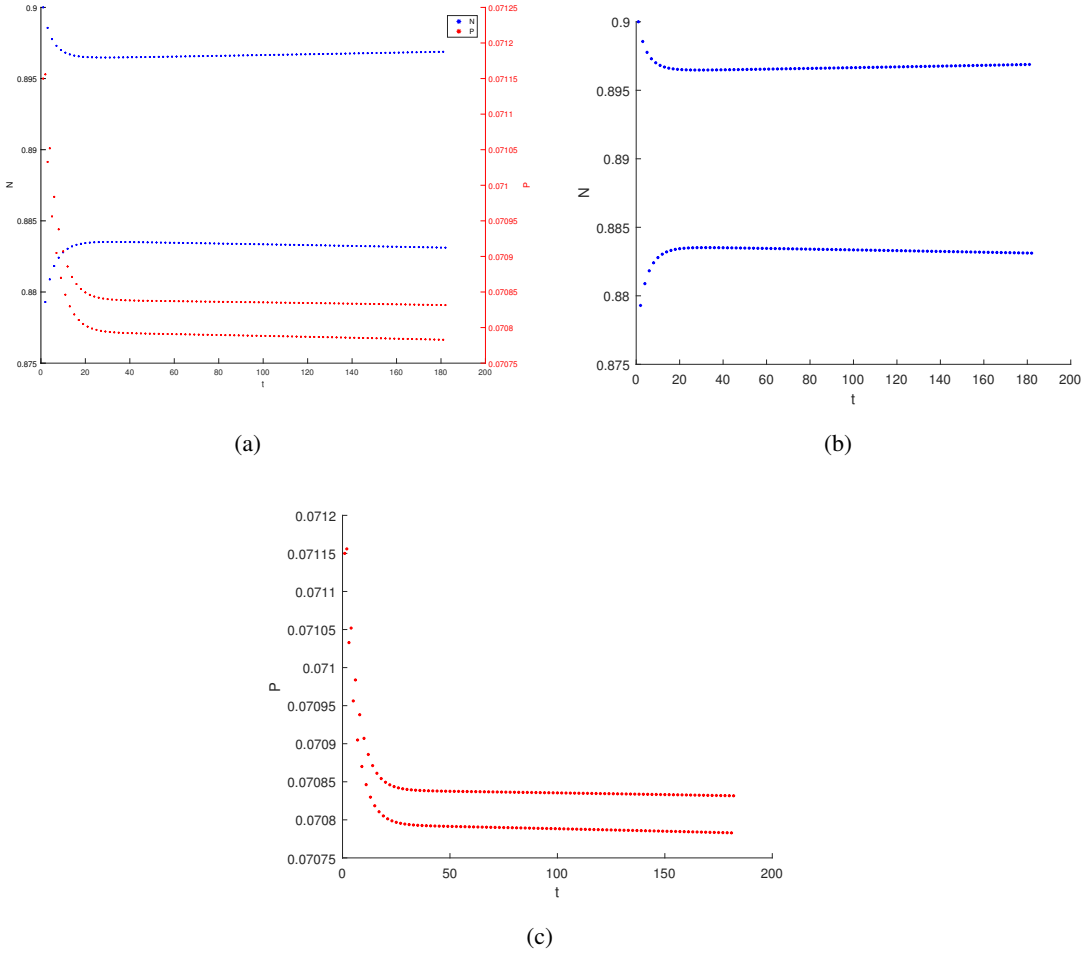

Figure 1. Flip bifurcation occurs at the equilibrium point $(N_0, P_0) \approx (0.89, 0.0708765)$. (a) is the comparison of the trend of variables N and P with the change over time t. (b) and (c) mark the period two bifurcation cases for both variables N and P, respectively.

4. Hopf bifurcation at E_4

In this section, we still choose h as the bifurcation parameter to discuss Hopf bifurcation around its positive equilibrium (N_0, P_0). The necessary conditions for Hopf bifurcation to occur is given by the following curve:

$$S = \left\{ (m, n, \theta, f, \epsilon) \in \mathbb{R}_+^5 : \ h = h_1^* = \frac{(2m-1-\theta)\left[1 + \sqrt{1+4f(1-m)(m-\theta)}\right]}{2(1-m)(m-\theta)\sqrt{1+4f(1-m)(m-\theta)}}, \ |E| < 2 \right\}$$

where $E = \frac{h}{\epsilon}\left(\frac{m(1+\theta-2m)}{1+\sqrt{1+4f(1-m)(m-\theta)}}\right) + 2$.

4.1. Existence condition of Hopf bifurcation at E_4

For emergence of Hopf bifurcation around positive equilibrium (N_0, P_0), two roots of the characteristic polynomial (2.2) must be complex conjugate with unit modulus. Therefore, it is easy to obtain the bifurcation parameter $h_1^* = \frac{(2m-\theta-1)\left(1+\sqrt{1+4f(1-m)(m-\theta)}\right)}{2(1-m)(m-\theta)\sqrt{1+4f(1-m)(m-\theta)}} > 0$, *i.e.*, $0 < m < \theta$ or $\frac{1+\theta}{2} < m < 1$.

We still consider parameter h with a small perturbation δ, and then characteristic equation (2.2) can be rewritten as:

$$\lambda^2 + p(\delta)\lambda + q(\delta) = 0,$$

where

$$p(\delta) = -\left[2 + \frac{\left(h_1^* + \delta\right)}{\epsilon}\left[\frac{2m(1+\theta-2m)}{n}\right]\right],$$

$$q(\delta) = 1 + \frac{\left(h_1^* + \delta\right)}{\epsilon}\left[\frac{2m(1+\theta-2m)}{n}\right] + \frac{\left(h_1^* + \delta\right)^2}{\epsilon}\left[\frac{m(n-1)(n-2)}{fn}\right]$$

The roots of the characteristic equation of $J|_{(N_0,P_0)}$ are

$$\lambda_1 = \frac{p(\delta) + i\sqrt{4q(\delta) - p(\delta)^2}}{2} \quad , \quad \lambda_2 = \frac{p(\delta) - i\sqrt{4q(\delta) - p(\delta)^2}}{2}$$

Also,

$$\left|\lambda_{1,2}\right| = \sqrt{q(\delta)} \quad , \quad \frac{d\left|\lambda_{1,2}\right|}{d\delta}|_{\delta=0} = \left[1 - \frac{4f(1+\theta-2m)^2}{\epsilon n(n-1)(n-2)} + \frac{2(2m-1-\theta)}{\epsilon mn}\right]^{-\frac{1}{2}} \frac{(1+\theta-2m)(m-2)}{\epsilon n}$$

where $\frac{d\left|\lambda_{1,2}\right|}{d\delta}|_{\delta=0} > 0$ if and only if $\frac{(1+\theta-2m)(m-2)}{\epsilon n} > 0$.

If $p(0) \neq 0, 1$, we have $-\frac{4f(2m-1-\theta)^2}{\epsilon n(n-1)(n-2)} \neq 2, 3$, which means $\lambda_{1,2}^n \neq 1$, $n = 1, 2, 3, 4$.

The transversal condition at (N_0, P_0) is given by

$$\begin{aligned}\frac{d|\lambda_1|^2}{d\delta}|_{\delta=0} &= \left(\lambda_1\frac{d\lambda_2}{d\delta} + \lambda_2\frac{d\lambda_1}{d\delta}\right)|_{\delta=0} \\ &= \frac{m(1+\theta-2m)}{\epsilon n}\left[3 + \frac{2mh_1^*(1+\theta-2m)}{\epsilon n}\right] + \frac{mh_1^*(n-1)(n-2)}{\epsilon fn}\end{aligned}$$

If $\frac{1+\theta}{2} < m < 1$, we have $\frac{d|\lambda_1|^2}{d\delta}|_{\delta=0} > 0$. Then, Hopf bifurcation will occur at (N_0, P_0).

4.2. The direction of Hopf bifurcation at E_4

Now, let

$$\alpha = 1 + \frac{h_1^*}{\epsilon}\left[\frac{m(1+\theta-2m)}{n}\right] \quad , \quad \beta = h_1^*\sqrt{\frac{m(n-1)(n-2)}{\epsilon fn} - \frac{m^2(1+\theta-2m)^2}{\epsilon^2 n^2}}$$

The invertible matrix T is given by

$$T = \begin{pmatrix} \frac{h}{\epsilon}\left[\frac{-2m(n-1)}{n}\right] & 0 \\ \alpha - 1 - \frac{h}{\epsilon}\left[\frac{2m(1+\theta-2m)}{n}\right] & -\beta \end{pmatrix}$$

Using the following translation

$$\begin{pmatrix} \overline{N_{n+1}} \\ \overline{P_{n+1}} \end{pmatrix} = T \begin{pmatrix} \overline{x_{n+1}} \\ \overline{y_{n+1}} \end{pmatrix}$$

Then, the Eq (3.4) transforms to

$$\begin{pmatrix} \overline{x_{n+1}} \\ \overline{y_{n+1}} \end{pmatrix} = \begin{pmatrix} \alpha & -\beta \\ \beta & \alpha \end{pmatrix} \begin{pmatrix} \bar{x}_n \\ \bar{y}_n \end{pmatrix} + \begin{pmatrix} f(\bar{x}_n, \bar{y}_n) \\ g(\bar{x}_n, \bar{y}_n) \end{pmatrix}$$

where

$$\begin{aligned}
&f(\bar{x}_n, \bar{y}_n) = l_{11}\bar{x}_n^2 + l_{12}\bar{x}_n\bar{y}_n + l_{13}\bar{y}_n^2 + l_{14}\bar{x}_n^3 + l_{15}\bar{x}_n^2\bar{y}_n + l_{16}\bar{x}_n\bar{y}_n^2 + l_{17}\bar{y}_n^3,\\
&g(\bar{x}_n, \bar{y}_n) = l_{21}\bar{x}_n^2 + l_{22}\bar{x}_n\bar{y}_n + l_{23}\bar{y}_n^2 + l_{24}\bar{x}_n^3 + l_{25}\bar{x}_n^2\bar{y}_n + l_{26}\bar{x}_n\bar{y}_n^2 + l_{27}\bar{y}_n^3,\\
&l_{11} = b_1\alpha^3 + b_2\alpha^2\beta + \alpha\beta^2 + b_3\alpha\beta^2, \quad l_{12} = -2b_1\alpha^2\beta + b_2\alpha^3 + \beta\alpha^2 - b_2\alpha\beta^2 - \beta^3 + 2b_3\alpha^2\beta,\\
&l_{13} = b_1\alpha\beta^2 - b_2\alpha^2\beta - \alpha\beta^2 + b_3\alpha^3, \quad l_{14} = b_4\alpha^4 + b_5\alpha^3\beta + b_6\alpha^2\beta^2 + b_7\alpha\beta^3,\\
&l_{15} = -3b_4\alpha^3\beta + b_5\alpha^4 - 2b_5\alpha^2\beta^2 + 2b_6\alpha^3\beta - b_6\alpha\beta^3 + 3b_7\alpha^2\beta^2,\\
&l_{16} = 3b_4\alpha^2\beta^2 + b_5\alpha\beta^3 - 2b_5\alpha^3\beta + b_6\alpha^4 - 2b_6\alpha^2\beta^2 + 3b_7\alpha^3\beta,\\
&l_{17} = -b_4\alpha\beta^3 + b_5\alpha^2\beta^2 - b_6\alpha^3\beta + b_7\alpha^4,\\
&l_{21} = b_1\alpha^2\beta + b_2\alpha\beta^2 - \alpha^2\beta + b_3\beta^3, \quad l_{22} = -2b_1\alpha\beta^2 + b_2\alpha^2\beta - b_2\beta^3 - \alpha^3 + \alpha\beta^2 + 2b_3\alpha\beta^2,\\
&l_{23} = b_1\beta^3 - b_2\alpha\beta^2 + \alpha^2\beta + b_3\alpha^2\beta, \quad l_{24} = b_4\alpha^3\beta + b_5\alpha^2\beta^2 + b_6\alpha\beta^3 + b_7\beta^4,\\
&l_{25} = -3b_4\alpha^2\beta^2 + b_5\alpha^3\beta - 2b_5\alpha\beta^3 + 2b_6\alpha^2\beta^2 - b_6\beta^4 + 3b_7\alpha\beta^3,\\
&l_{26} = 3b_4\alpha\beta^3 + b_5\beta^4 - 2b_5\alpha^2\beta^2 + b_6\alpha^3\beta - 2b_6\alpha\beta^3 + 3b_7\alpha^2\beta^2,\\
&l_{27} = -b_4\beta^4 + b_5\alpha\beta^3 - b_6\alpha^2\beta^2 + b_7\alpha^3\beta
\end{aligned}$$

Next, by using the center manifold theorem and normal form theories, the direction of Hopf bifurcation at E_4 is given. According to the normal form theories related to bifurcation analysis, we require the following quantity at $(x, y, \delta) = (0, 0, 0)$.

$$L = -\mathrm{Re}\left[\frac{(1-2\lambda)\,\bar{\lambda}^2}{1-\lambda}\xi_{11}\xi_{20}\right] - \frac{1}{2}|\xi_{11}|^2 - |\xi_{02}|^2 + \mathrm{Re}\left(\bar{\lambda}\xi_{21}\right)$$

where

$$\begin{aligned}
&\xi_{20} = \frac{1}{8}\left[f_{\bar{x}\bar{x}} + f_{\bar{y}\bar{y}} + 2g_{\bar{x}\bar{y}} + i\left(g_{\bar{x}\bar{x}} - g_{\bar{y}\bar{y}} - 2f_{\bar{x}\bar{y}}\right)\right], \quad \xi_{11} = \frac{1}{4}\left[f_{\bar{x}\bar{x}} + f_{\bar{y}\bar{y}} + i\left(g_{\bar{x}\bar{x}} + g_{\bar{y}\bar{y}}\right)\right],\\
&\xi_{02} = \frac{1}{8}\left[f_{\bar{x}\bar{x}} - f_{\bar{y}\bar{y}} + 2g_{\bar{x}\bar{y}} + i\left(g_{\bar{x}\bar{x}} - g_{\bar{x}\bar{y}} + 2f_{\bar{x}\bar{y}}\right)\right],\\
&\xi_{21} = \frac{1}{16}\left[f_{\bar{x}\bar{x}\bar{x}} + f_{\bar{x}\bar{y}\bar{y}} + g_{\bar{x}\bar{x}\bar{y}} + g_{\bar{y}\bar{y}\bar{y}} + i\left(g_{\bar{x}\bar{x}\bar{x}} + g_{\bar{x}\bar{y}\bar{y}} - f_{\bar{x}\bar{x}\bar{y}} - f_{\bar{y}\bar{y}\bar{y}}\right)\right],\\
&f_{\bar{x}\bar{x}} = 2l_{11}\ ,\ f_{\bar{x}\bar{y}} = l_{12}\ ,\ f_{\bar{x}\bar{x}\bar{x}} = 6l_{14}\ ,\ f_{\bar{x}\bar{x}\bar{y}} = 2l_{15}\ ,\ f_{\bar{x}\bar{y}\bar{y}} = 2l_{16}\ ,\ f_{\bar{y}\bar{y}} = 2l_{13}\ ,\ f_{\bar{y}\bar{y}\bar{y}} = 6l_{17},\\
&g_{\bar{x}\bar{x}} = 2l_{21}\ ,\ g_{\bar{x}\bar{y}} = l_{22}\ ,\ g_{\bar{x}\bar{x}\bar{x}} = 6l_{24}\ ,\ g_{\bar{x}\bar{x}\bar{y}} = 2l_{25}\ ,\ g_{\bar{x}\bar{y}\bar{y}} = 2l_{26}\ ,\ g_{\bar{y}\bar{y}} = 2l_{23}\ ,\ g_{\bar{y}\bar{y}\bar{y}} = 6l_{27}\ .
\end{aligned}$$

Theorem 4.1. *If the above conditions hold, and $L \neq 0$, the Hopf bifurcation occurs at the point (N_0, P_0). When $\delta > 0$, if $L < 0$, then it attracts at that point; when $\delta < 0$, if $L > 0$, then it repels at that point.*

To verify whether the condition is correct, we select the following parameters for numerical simulations and obtain the following conclusions. By selecting the first set of parameters $h \approx 0.062163$, $e = 1$, $\theta = 0.1$, $f = 1$, $m = 0.554$, the unique positive equilibrium point $(N_0, P_0) \approx (0.554, 0.004932)$ of the model can be obtained. By choosing the initial value $K_1 = (0.5, 0.005)$, the following results can be obtained by numerical simulation.

Figure 2 reflects that variable N gradually tends to oscillate steadily at the equilibrium point $N = 0.554$ with the increase of the number of iterations n, while variable P also gradually oscillates steadily with the increase of the number of iterations N, but the equilibrium point is attracted to $P \approx 0.157$.

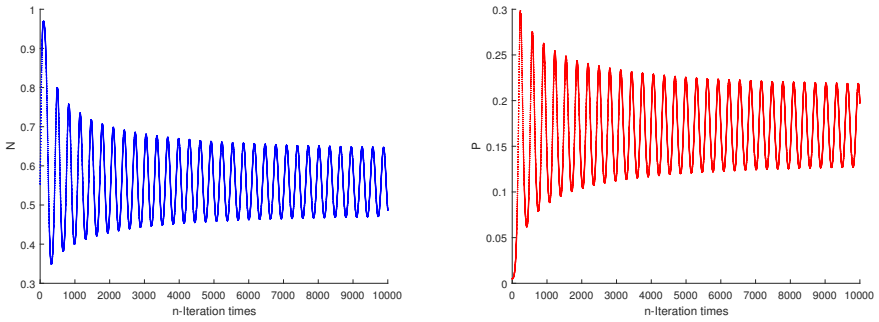

(a) (b)

Figure 2. Hopf bifurcation occurs at the equilibrium point $(N_0, P_0) \approx (0.554, 0.004932)$. (a) and (b) are the variations of N,P with the number of iterations n, respectively.

By choosing the second set of parameters $h \approx 1.120901$, $e = 1$, $\theta = 0.61$, $f = 1$, $m = 0.823$ the only internal equilibrium point $(N_0, P_0) \approx (0.823, 0.020442)$ of the model can be obtained. Choosing the initial value $K_2 = (0.8, 0.02)$, the following results can be obtained by numerical simulation.

Figure 3 shows that as the number of iterations n increases, eventually, the variable P will also be attracted to stabilize at $P \approx 0.035$.

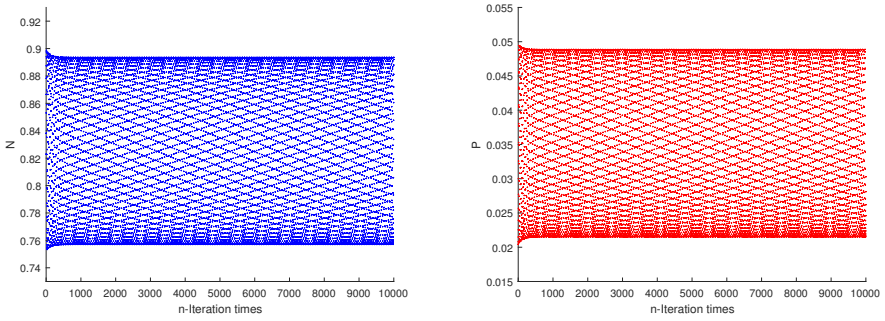

(a) (b)

Figure 3. Hopf bifurcation occurs at the equilibrium point $(N_0, P_0) \approx (0.823, 0.020442)$. (a) and (b) are the variations of N,P with the number of iterations n, respectively.

5. Chaos analysis

In this section, chaotic cases at bifurcating points are analyzed using numerical simulations. We give maximum Lyapunov exponents and phase diagrams for different perturbation parameters to prove our results. The chaos theory analysis of Flip bifurcation and Hopf bifurcation is given as follows.

Definition 5.1. [27] *The formula for the maximum Lyapunov index is given by*

$$\lambda = \lim_{n\to\infty} \frac{1}{n} \sum_{n=0}^{n-1} \ln \left| \frac{df(x_n, \mu)}{dx} \right|$$

Theorem 5.1. [27] *If $\lambda < 0$, the neighboring points eventually come together and merge into a single point, which corresponds to stable immobile points and periodic motion. If $\lambda > 0$, the neighboring points eventually separate, which corresponds to local instability of the orbit generating chaotic situations.*

In the following, we choose two different equilibria to consider the Flip bifurcation with chaotic cases. Initially, we select the parameters $h = 0.95$, $e \approx 0.1841359$, $\theta = 0.5$, $f = 1$, $m = 0.961$, and obviously the model comes to

$$\begin{cases} N_{n+1} = N_n + 0.95 \left\{ \frac{1}{0.1841359} \left[N_n (1 - N_n) (N_n - 0.5) \frac{1}{1+P_n} - N_n P_n \right] \right\} \\ P_{n+1} = P_n + 0.95 \left[N_n P_n - 0.961 P_n \right] \end{cases}$$

where the internal equilibrium point is $(N_1, P_1) \approx (0.961, 0.01807)$.

After selecting the perturbation $\delta \in (0, 0.2)$ and analyzing the trend of N with δ by numerical simulation, we obtain the chaotic bifurcating cases (see Figure 4).

Next, choosing the parameters $h = 0.95$, $e \approx 0.184136$, $\theta = 0.5$, $f = 1$, $m = 0.9601$, we obtain the model

$$\begin{cases} N_{n+1} = N_n + 0.95 \left\{ \frac{1}{0.184136} \left[N_n (1 - N_n) (N_n - 0.5) \frac{1}{1+P_n} - N_n P_n \right] \right\} \\ P_{n+1} = P_n + 0.95 \left[N_n P_n - 0.9601 P_n \right] \end{cases}$$

Obviously, the internal equilibrium point $(N_2, P_2) \approx (0.9601, 0.0180734)$. We still choose the perturbation $\delta \in (0, 0.2)$ to analyze the trend of N with δ. The chaotic bifurcating case is obtained (see Figure 5). By calculating the bifurcating diagrams and the maximum Lyapunov exponent for two bifurcating points with small differences, it can be shown that the small change of the initial value near the equilibrium point has a great influence on the stability of the initial state. Although they are different perturbed bifurcating cases, the two cases tend to go the same during the process of δ gradually increasing.

In the following, we choose two different equilibria to consider Hopf bifurcation with chaotic cases. By picking the first set of parameters $h \approx 0.062163$, $e = 1$, $\theta = 0.1$, $f = 1$, $m = 0.554$, the unique internal equilibrium point $(N_3, P_3) \approx (0.554, 0.004932)$ of the model can be obtained.

After choosing perturbation $\delta \in (0, 0.5)$, we obtain phase diagrams (see Figure 6).

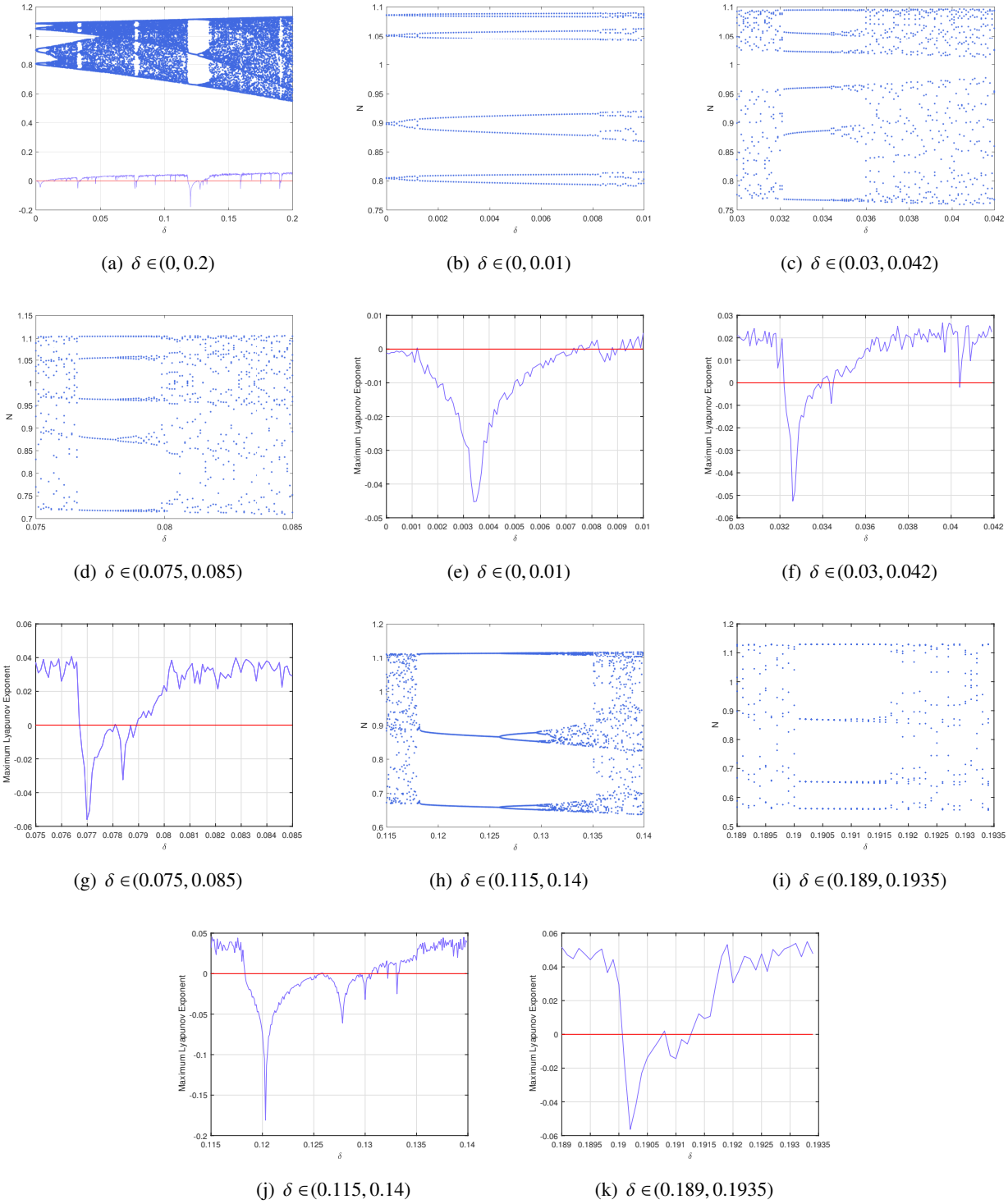

(a) $\delta \in (0, 0.2)$ (b) $\delta \in (0, 0.01)$ (c) $\delta \in (0.03, 0.042)$

(d) $\delta \in (0.075, 0.085)$ (e) $\delta \in (0, 0.01)$ (f) $\delta \in (0.03, 0.042)$

(g) $\delta \in (0.075, 0.085)$ (h) $\delta \in (0.115, 0.14)$ (i) $\delta \in (0.189, 0.1935)$

(j) $\delta \in (0.115, 0.14)$ (k) $\delta \in (0.189, 0.1935)$

Figure 4. $\delta \in (0, 0.2)$-bifurcation diagrams at point $(N_1, P_1) \approx (0.961, 0.01807)$ compared with maximum Lyapunov exponent. (a) indication that in the range of $\delta \in (0, 0.2)$, the bifurcation diagram corresponds to the maximum Lyapunov exponent. The accuracy of the conclusions can be seen by comparing bifurcation amplifications and the maximum Lyapunov exponent amplifications in the same range of δ from (b) to (k).

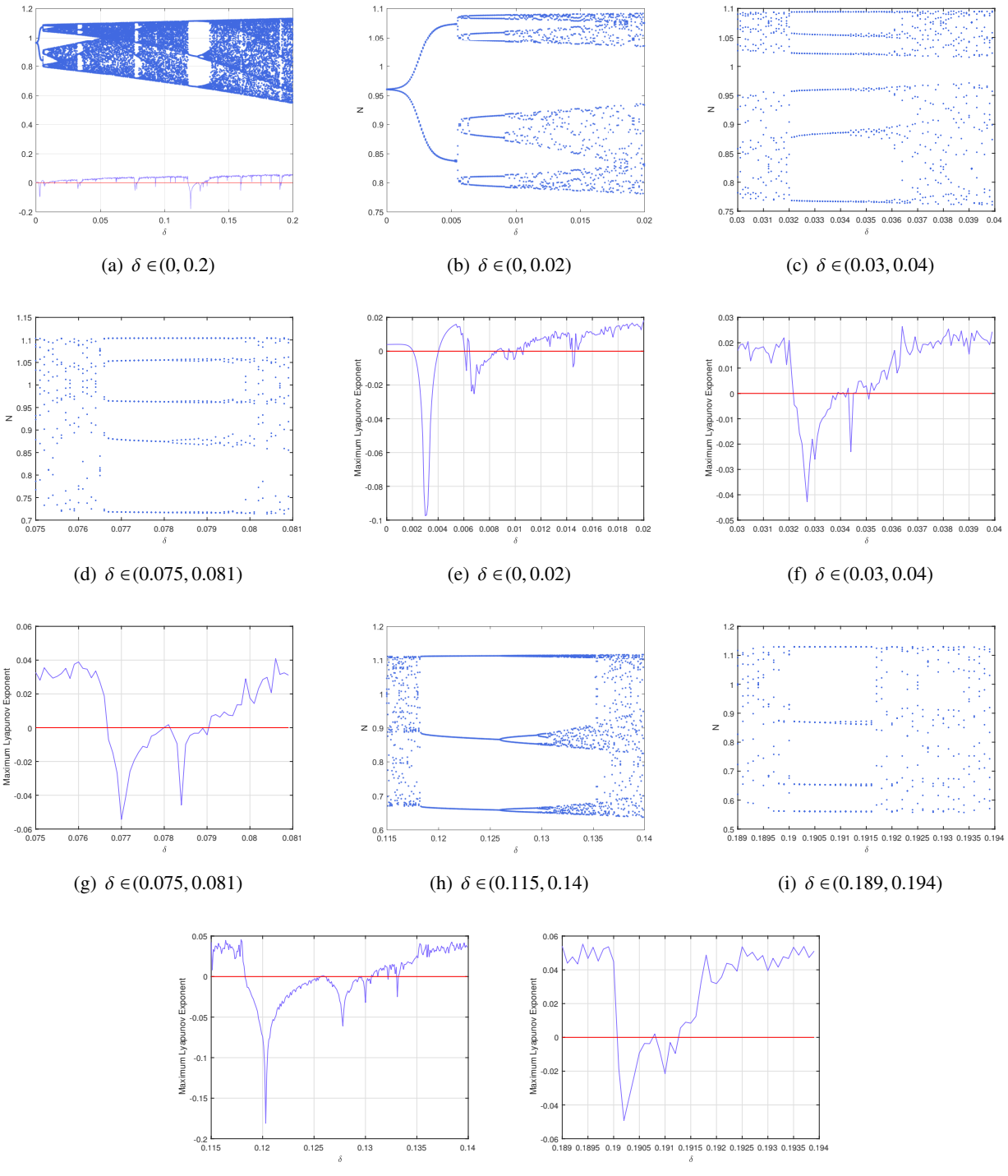

(a) $\delta \in (0, 0.2)$ (b) $\delta \in (0, 0.02)$ (c) $\delta \in (0.03, 0.04)$

(d) $\delta \in (0.075, 0.081)$ (e) $\delta \in (0, 0.02)$ (f) $\delta \in (0.03, 0.04)$

(g) $\delta \in (0.075, 0.081)$ (h) $\delta \in (0.115, 0.14)$ (i) $\delta \in (0.189, 0.194)$

(j) $\delta \in (0.115, 0.14)$ (k) $\delta \in (0.189, 0.194)$

Figure 5. $\delta \in (0, 0.2)$-bifurcation diagrams at point $(N_2, P_2) \approx (0.9601, 0.0180734)$ compared with maximum Lyapunov exponent. (a) indication that in the range of $\delta \in (0, 0.2)$, the bifurcation diagram corresponds to the maximum Lyapunov exponent. The accuracy of the conclusions can be seen by comparing bifurcation amplifications and the maximum Lyapunov exponent amplifications in the same range of δ from (b) to (k).

The analysis mentioned above shows that with the perturbation δ increasing, the asymptotic stability of variable N gradually becomes weaker, and the range of periodic solutions gradually becomes larger, but the convergence speed comes faster increases (see Figure 6).

By choosing the second set of parameters $h \approx 1.120901$, $e = 1$, $\theta = 0.61$, $f = 1$, $m = 0.823$, we can obtain the unique internal equilibrium point $(N_4, P_4) \approx (0.823, 0.020442)$ of the model.

After choosing perturbation $\delta \in (-1, 1)$, we obtain phase diagrams (see Figure 7).

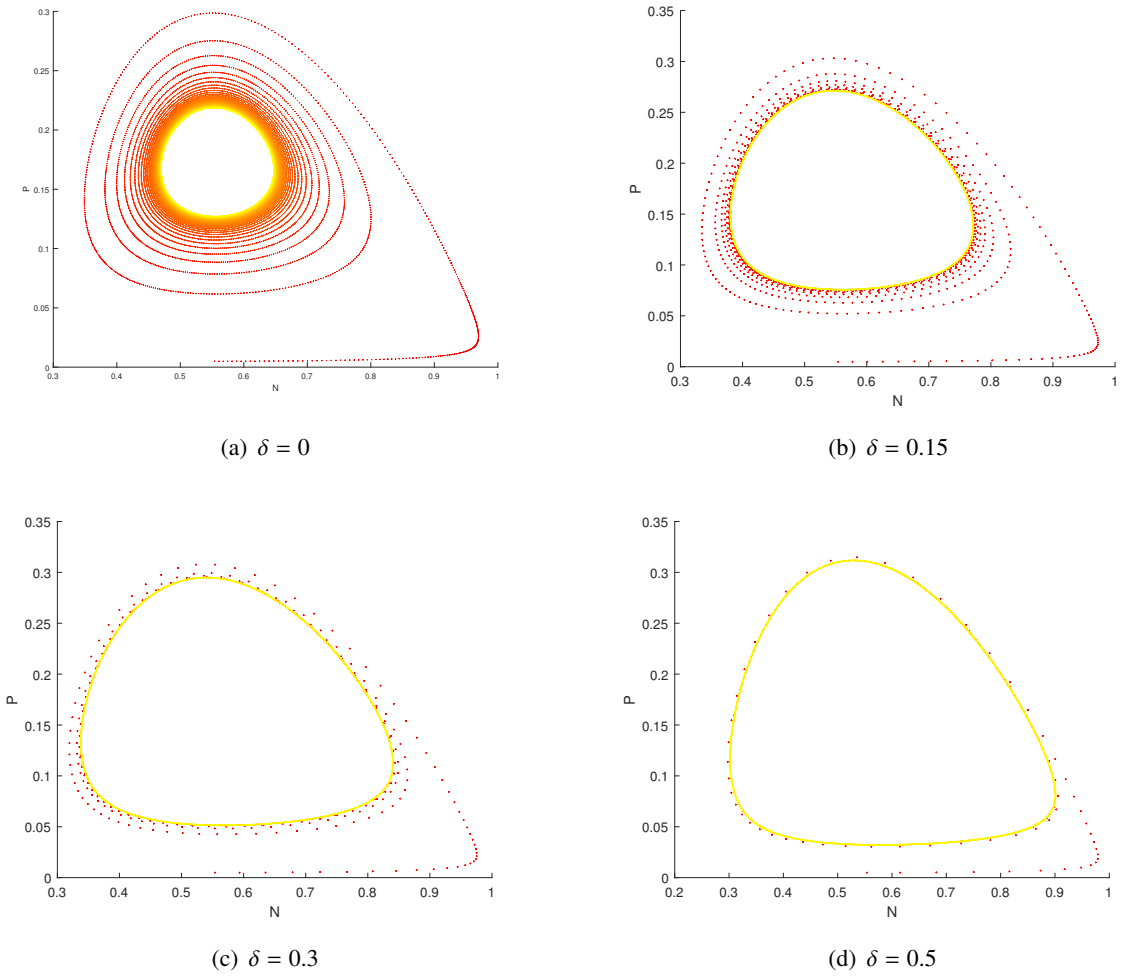

(a) $\delta = 0$ (b) $\delta = 0.15$

(c) $\delta = 0.3$ (d) $\delta = 0.5$

Figure 6. Phase diagrams under different perturbations at the equilibrium point $(N_3, P_3) \approx (0.554, 0.004932)$. (a) indicates that N will slowly stabilize without perturbation. (b), (c) and (d) show that the rate of convergence to stability will become faster with increasing δ. No chaotic situations occur.

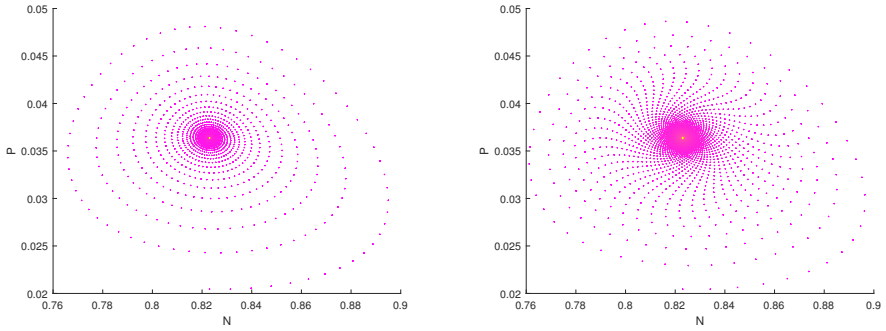

(a) $\delta = -0.5$ (b) $\delta = -0.3$

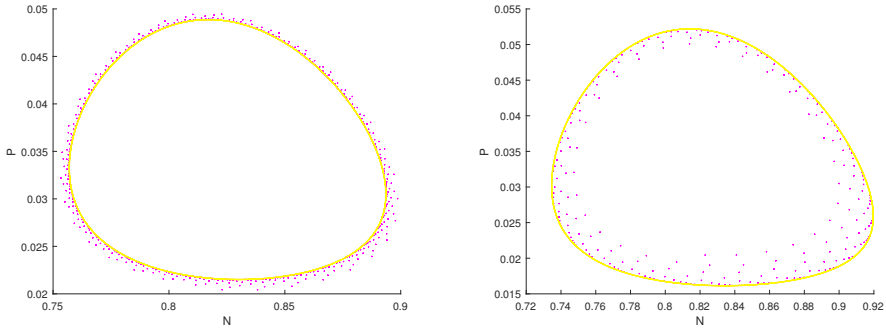

(c) $\delta = 0$ (d) $\delta = 0.2$

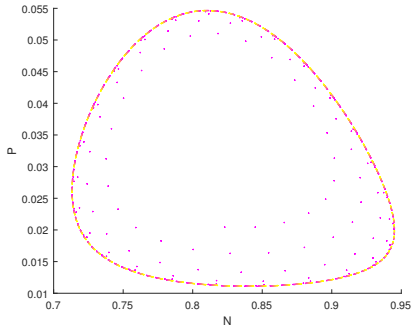

(e) $\delta = 0.5$

Figure 7. Phase diagrams under different perturbations at the equilibrium point $(N_4, P_4) \approx (0.823, 0.020442)$. (a) and (b) tend to stabilize at a center point. However, (c), (d), and(e) are stable in a orbit. No chaotic situations occur.

6. Conclusions

Our work deals with the study of local dynamical properties of a predator-prey model with discrete time (1.2), Flip bifurcation and Hopf bifurcation associated with the periodic solution, as well as their chaotic cases. We prove that the system (1.2) has four unique equilibria. In addition, their stability and instability conditions are given, which mark the final equilibrium state of both groups as fear, climate and other factors change. We focus on the unique positive equilibrium point

$E_4 = \left(m, \frac{-1+\sqrt{1+4f(1-m)(m-\theta)}}{2f}\right)$, with stability condition:

$$\begin{cases} 1 + \frac{h}{\epsilon}\left[\frac{m(1+\theta-2m)}{1+\sqrt{1+4f(1-m)(m-\theta)}}\right] + \frac{h^2}{\epsilon}\left[\frac{m(1-m)(m-\theta)\sqrt{1+4f(1-m)(m-\theta)}}{\left[1+\sqrt{1+4f(1-m)(m-\theta)}\right]^2}\right] > 0 \\ m(1-m)(m-\theta)\sqrt{1+4f(1-m)(m-\theta)} > 0 \\ \frac{1+\theta-2m}{1+\sqrt{1+4f(1-m)(m-\theta)}} + h\left[\frac{2(1-m)(m-\theta)\sqrt{1+4f(1-m)(m-\theta)}}{\left[1+\sqrt{1+4f(1-m)(m-\theta)}\right]^2}\right] < 0 \end{cases}$$

Significantly, after analyzing the formation conditions of Flip bifurcation and Hopf bifurcation at (N_0, P_0), we give their chaotic scenarios from both theoretical and numerical simulations. Moreover, it is found that Flip bifurcation is more prone to chaos scenarios, and Hopf bifurcation is closely related to periodic solutions.

Biologically, the occurrence of Flip bifurcation implies the number of predators and prey will alternate around a value instead of converging to a fixed value, eventually. The corresponding chaotic scenario suggests that small perturbations in the variable parameters will eventually have a significant impact on the population, ultimately leading to chaos. The appearance of Hopf bifurcation points indicates that the equilibrium point of the system loses its attraction and eventually produces a closed orbit, which implies the existence of periodic oscillations of predators and prey. Therefore, we can precisely change the biological density of predators and prey to achieve the desired goal by regulating the number of bifurcation parameters h, for the fact that the chaotic scenario does not exist. All the conclusions illustrate the effect of fear on populations. Finally, the accuracy of the theory is demonstrated using the maximum Lyapunov exponent and phase diagrams.

In future work, the model can be investigated using different discrete methods. In addition, to obtain specific biological properties, new bifurcation parameters can be selected for the study to obtain the desired conclusions.

Conflict of interest

The authors declare that they have no competing interests.

References

1. X. L. Liu, D. M. Xiao, Bifurcations in a discrete time lotka-volterra predator-prey system, *Discrete Cont. Dyn. Syst. B*, **6** (2012), 559–572. http://doi.org/10.3934/dcdsb.2006.6.559
2. Z. M. He, X. Lai, Bifurcation and chaotic behavior of a discrete-time predator-prey system, *Nonlinear Anal.*, **12** (2011), 403–417. http://doi.org/10.1016/j.nonrwa.2010.06.026
3. X. Y. Li, X. M. Shao, Flip bifurcation and Neimark-Sacker bifurcation in a discrete predator-prey model with Michaelis-Menten functional response, *Electron. Res. Arch.*, **31** (2022), 37–57. http://doi.org/10.3934/era.2023003
4. L. F. Cheng, H. J. Cao, Bifurcation analysis of a discrete-time ratio-dependent predator-prey model with Allee effect, *Commun. Nonlinear Sci. Numer. Simulat.*, **38** (2016), 288–302. http://doi.org/10.1016/j.cnsns.2016.02.038

5. B. H. Hong, C. R. Zhang, Neimark-Sacker bifurcation of a discrete-time predator-prey model with prey refuge effect, *Mathematics*, **11** (2023), 1399. https://doi.org/10.3390/math11061399
6. T. S. Huang, H. Y. Zhang, Bifurcation, chaos and pattern formation in a space- and time-discrete predator-prey system, *Chaos Soliton. Fract.*, **91** (2016), 92–107. http://doi.org/10.1016/j.chaos.2016.05.009
7. K. Nadjah, A. M. Salah, Stability and Hopf bifurcation of the coexistence equilibrium for a differential-algebraic biological economic system with predator harvesting, *Electron. Res. Arch.*, **29** (2020), 1641–1660. http://doi.org/10.3934/era.2020084
8. H. Y. Chen, C. R. Zhang, Bifurcations and hydra effects in a reaction-diffusion predator-prey model with Holling II functional response, *J. Appl. Anal. Comput.*, **13** (2023), 424–444. http://doi.org/10.11948/20220221
9. W. Li, X. Y. Li, Neimark-Sacker bifurcation of a semi-discrete hematopoiesis model, *J. Appl. Anal. Comput.*, **8** (2018), 1679–1693. http://doi.org/10.11948/2018.1679
10. C. Liu, Q. L. Zhang, J. Huang, W. S. Tang, Dynamical behavior of a harvested prey-predator model with stage structure and discrete time delay, *J. Biol. Syst.*, **17** (2009), 759–777. http://doi.org/10.1142/S0218339009002995
11. A. Singh, P. Malik, Bifurcations in a modified Leslie-Gower predator-prey discrete model with Michaelis-Menten prey harvesting, *J. Appl. Math. Comput.*, **67** (2021), 143–174. http://doi.org/10.1007/s12190-020-01491-9
12. S. M. Salman, A. M. Yousef, A. M. Elsadany, Stability, bifurcation analysis and chaos control of a discrete predator-prey system with square root functional response, *Chaos Soliton. Fract.*, **93** (2016), 20–31. http://doi.org/10.1016/j.chaos.2016.09.020
13. E. Van Velzen, U. Gaedke, Disentangling eco-evolutionary dynamics of predator-prey coevolution: the case of antiphase cycles, *Sci. Rep.*, **7** (2017), 17125. http://doi.org/10.1038/s41598-017-17019-4
14. Z. K. Huang, X. H. Wang, Y. H. Xia, A predator-prey system with anorexia response, *Nonlinear Anal.*, **8** (2007), 1–19. http://doi.org/10.1016/j.nonrwa.2005.05.004
15. S. Ruan, On nonlinear dynamics of predator-prey models with discrete delay, *Math. Model. Nat. Phenom.*, **4** (2009), 140–188. http://doi.org/10.1051/mmnp/20094207
16. H. Y. Chen, C. R. Zhang, Dynamic analysis of a Leslie-Gower-type predator-prey system with the fear effect and ratio dependent Holling III functional response, *Nonlinear Anal.-Model.*, **27** (2022), 904–926. http://doi.org/10.15388/namc.2022.27.27932
17. D. R. Brown, T. W. Sherry, Food supply controls the body condition of a migrant bird wintering in the tropics, *Oecologia*, **149** (2006), 22–32. http://doi.org/10.1007/s00442-006-0418-z
18. X. X. Liu, C. R. Zhang, Stability and optimal control of tree-insect model under forest fire disturbance, *Mathematics*, **10** (2022), 2563. http://doi.org/10.3390/math10152563
19. X. Y. Wang, L. Zanette, X. F. Zou, Modelling the fear effect in predator-prey interactions, *J. Math. Biol.*, **73** (2016), 1179–1204. http://doi.org/10.1007/s00285-016-0989-1

20. S. K. Sasmal, Population dynamics with multiple allee effects induced by fear factors – a mathematical study on prey-predator interactions, *Appl. Math. Model.*, **64** (2018), 1–14. http://doi.org/10.1016/j.apm.2018.07.021

21. X. L. Liu, D. M. Xiao, Complex dynamic behaviors of a discrete-time predator-prey system, *Chaos Solition. Fract.*, **32** (2007), 80–94. http://doi.org/10.1016/j.chaos.2005.10.081

22. A. Q. Khan, Supercritical Neimark-Sacker bifurcation of a discrete-time Nicholson-Bailey model, *Math. Method. Appl. Sci.*, **41** (2018), 4841–4852. http://doi.org/10.1002/mma.4934

23. Y. Li, M. Rafaqat, T. J. Zia, I. Ahmed, C. Y. Jung, Flip and Neimark-Sacker bifurcations of a discrete time predator-pre model, *IEEE Access*, **7** (2019), 123430–123435. http://doi.org/10.1109/ACCESS.2019.2937956

24. Z. H. Yu, L. Li, W. M. Zhang, Dynamic behaviors of a symmetrically coupled period-doubling system, *J. Math. Anal. Appl.*, **512** (2022), 126189. http://doi.org/10.1016/j.jmaa.2022.126189

25. J. L. Chen, Y. M. Chen, Z. L. Zhu, F. D. Chen, Stability and bifurcation of a discrete predator-prey system with Allee effect and other food resource for the predators, *J. Appl. Math. Comput.*, **69** (2022), 529–548. http://doi.org/10.1007/s12190-022-01764-5

26. B. D. Zheng, L. J. Liang, C. R. Zhang, Extended Jury criterion, *Sci. China Math.*, **53** (2010), 1133–1150. http://doi.org/10.1007/s11425-009-0208-2

27. L. M. Pecora, T. L. Carroll, Synchronization in chaotic systems, *Phys. Rev. Lett.*, **64** (1990), 821–824. http://doi.org/10.1103/PhysRevLett.64.821

AIMS Press